4th WSEAS International Conference on ELECTRONICS, CONTROL and SIGNAL PROCESSING, Miami, Florida, USA, 17-19 November, 2005 (pp.29-34)

Adaptive Filtering Using Filter Banks and Sparse Subfilters

PAULO B. BATALHEIRO
State University of Rio de Janeiro
Electronics and Telecomm. Eng. Depart.
20550-013, Rio de Janeiro, RJ
BRAZIL

MARIANE R. PETRAGLIA, ANTONIO PETRAGLIA
Federal University of Rio de Janeiro
Electronics Eng. Depart./Poli, PEE/COPPE
CP 68504, 21945-970, Rio de Janeiro, RJ
BRAZIL

Abstract: Some convergence properties of an adaptive filter structure which employs an analysis filter bank and sparse adaptive subfilters are investigated in this paper. By properly choosing the filter bank and the number of adaptive coefficients, such a structure is capable of modeling any linear system with finite impulse response (FIR). Using the analysis results derived in this paper, an optimization procedure is described to select the prototype filter of a cosine modulated filter bank that results in the best convergence rate for a given input signal statistics. The convergence behavior of the proposed subband adaptation algorithm is verified by computer simulations and compared to the behavior of previously proposed algorithms. It is shown that significant improvement in the convergence rate can be obtained with the sparse subband structure using very simple filter banks, when compared to the conventional direct-form LMS algorithm, for colored input signals.

Key–Words: Adaptive filtering, Filter banks, Filter design, Convergence analysis, Multirate processing.

1 Introduction

Adaptive algorithms that make use of transforms and filter banks have been proposed recently [1]-[12] with the objective of improving the convergence rate of the least-mean square (LMS) algorithm for colored input signals with no significant increase in the computational complexity. Two classes of adaptive filter bank structures have been reported. In the first one, the adaptation and filtering are performed at the reduced sampling rate [1]-[7], which leads to savings in the computational complexity for high-order adaptive filters. In the second one, the sampling rates of the signals inside the structures are not changed, resulting in a filter structure composed of a parallel connection of adaptive subfilters [8]-[11] as illustrated in Fig. 1.

The transform-domain LMS algorithm [8] was one of the first algorithms applying a transform to the input vector before processing it. In such an algorithm, the transform (usually a DCT or a DFT) corresponds to a simple analysis bank (with filters of length M for an M-band structure) and only one adaptive coefficient is used in each subband. The good performance of the transform-domain LMS algorithm, however, relies on the proper choice of the transform employed, which requires accurate information about the input signal model. The transform-domain structure was extended in [9], where sparse adaptive subfilters were used in the subbands. In [10] and [11], better analysis filters (of length larger than M) were used.

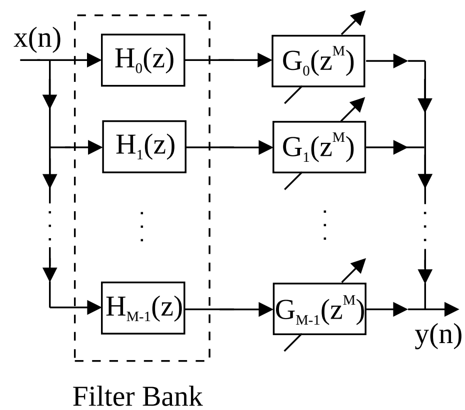

Figure 1: Adaptive structure using an analysis filter bank and sparse subfilters.

The better selectivity of longer analysis filters, when compared to those of a transform-based bank, can lead to a significant reduction in the convergence time for colored input signals.

The structure of Fig. 1 was believed to be able to implement only a subclass of FIR systems [11]. In Section 2 we show that, by properly choosing the filter bank and the number of coefficients of the adaptive subfilters, the structure of Fig. 1 becomes capable of modeling any FIR system, except for the introduction of an extra input-output delay. The coefficients of the subfilters are adapted by a normalized LMS-type algorithm, also described in Section 2. The adaptation convergence rate of the sparse subband structure is analyzed in Section 3. In Section 4, an optimization procedure for the design of the filter bank of the structure of Fig. 1 is described. Computer simulations in system identification and acoustic echo cancellation are presented in Section 5, where the convergence behavior of the proposed adaptive subband structure is compared to those of the conventional LMS and generalized transform-domain LMS algorithms. In Section 6, the concluding remarks are presented.

2 Adaptive Filter Bank Structure with Sparse Subfilters

The filter bank structure with adaptive sparse subfilters depicted in Fig. 1 can be redrawn as shown in Fig. 2 by making use of the polyphase representation of the analysis filter bank [13]. From Fig. 2, the trans-

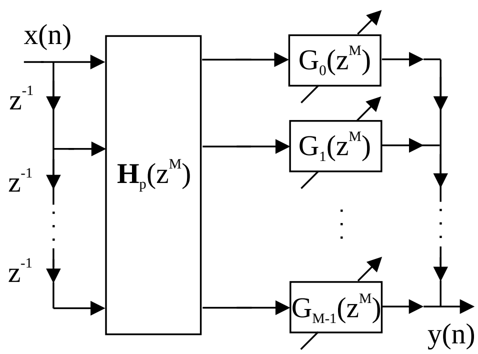

Figure 2: Adaptive structure of Fig. 1 with polyphase representation of the filter bank.

fer function implemented by the adaptive structure of Fig. 1 is

$$W(z)=\left[G_0(z^M)\cdots G_{M-1}(z^M)\right]\boldsymbol{H}_p(z^M)\begin{bmatrix}1\\ z^{-1}\\ \vdots\\ z^{-(M-1)}\end{bmatrix}, \tag{1}$$

where $\boldsymbol{H}_p(z) = [H_{i,j}(z)]$ is the filter bank type 1 polyphase matrix, with $H_{i,j}(z)$ being the jth polyphase component of the ith analysis filter $H_i(z)$, that is,

$$H_i(z) = \sum_{j=0}^{M-1} z^{-j} H_{i,j}(z^M). \tag{2}$$

In a system identification application, the coefficients of the subfilters $G_i(z^M)$ are adapted such as to model an unknown FIR system, denoted here by $S(z)$. The unknown system transfer function $S(z)$ can be expressed in terms of its polyphase components $(S_0(z), S_1(z), \cdots, S_{M-1}(z))$ as

$$S(z)=\left[S_0(z^M)\ S_1(z^M)\cdots S_{M-1}(z^M)\right]\begin{bmatrix}1\\ z^{-1}\\ \vdots\\ z^{-(M-1)}\end{bmatrix}. \tag{3}$$

From Eqs. (1) and (3), the subband structure models exactly the unknown FIR system $S(z)$ when

$$\left[G_0(z^M)\quad G_1(z^M)\quad\cdots\quad G_{M-1}(z^M)\right] = \left[S_0(z^M)\ S_1(z^M)\cdots S_{M-1}(z^M)\right][\boldsymbol{H}_p(z^M)]^{-1}. \tag{4}$$

Such equality cannot be achieved, in general, with causal FIR subfilters $G_i(z^M)$, since the elements of the matrix $[\boldsymbol{H}_p(z^M)]^{-1}$ are non-causal and/or IIR. However, if

$$\left[G_0(z^M)\quad G_1(z^M)\quad\cdots\quad G_{M-1}(z^M)\right] = \left[S_0(z^M)\quad S_1(z^M)\quad\cdots\quad S_{M-1}(z^M)\right]\boldsymbol{F}_p(z^M) \tag{5}$$

with $\boldsymbol{F}_p(z)$ such that

$$\boldsymbol{F}_p(z)\boldsymbol{H}_p(z) = z^{-m_0}\begin{bmatrix} & \boldsymbol{I}_{M-r}\\ z^{-1}\boldsymbol{I}_r & \end{bmatrix}, \tag{6}$$

for some integer r with $0 \leq r \leq M-1$, some integer m_0, and with $\boldsymbol{I}_k$ the $k \times k$ identity matrix, the transfer function implemented by the structure of Fig. 1 will be

$$W(z) = S(z)z^{-\Delta} = S(z)z^{-(m_0 M + r)}. \tag{7}$$

The matrices $\boldsymbol{H}_p(z)$ and $\boldsymbol{F}_p(z)$ that satisfy Eq. (6) correspond, respectively, to the analysis and synthesis polyphase matrices of a perfect reconstruction multirate system. Therefore, by using an analysis filter bank which yields perfect reconstruction and adaptive subfilters of sufficient order to satisfy Eq. (5), the structure of Fig. 1 implements exactly any FIR system.

For an M-band adaptive structure with analysis and synthesis filters of length N_P, the delay introduced by the filter bank, which must be taken into account in the adaptation algorithm, is $\Delta = m_0 M + r = N_P - M + r$. In order to satisfy Eq. (5), the number of adaptive coefficients of the subfilters $G_i(z)$ should be at least $K = \lceil (N_S + N_P)/M \rceil - 1$, where N_S is the length of the unknown system.

2.1 Adaptation Algorithm

A normalized LMS algorithm is used for updating the coefficients of the subfilters. Denoting $x_i(n)$ as the signal at the output of the ith analysis filter and $g_{i,k}$ as the kth coefficient of the subfilter $G_i(z)$, the general form for the LMS adaptation algorithm that minimizes the overall mean-square error is

$$g_{i,k}(n) = g_{i,k}(n-1) + \mu_i(n)e(n)x_i(n-Mk), \quad (8)$$

for $i = 0, 1, \cdots, M-1$ and $k = 0, 1, \cdots, K-1$. In the above equation, the error signal $e(n)$ is given by

$$e(n) = d(n-\Delta) - y(n), \quad (9)$$

where $d(n)$ is the desired response, $y(n)$ is the output of the adaptive subband structure, and Δ is the delay introduced by the filter bank (see Eq. (7)). The step-size for each subfilter can be made inversely proportional to the power of the corresponding transformed signal, i.e., $\mu_i(n) = \mu/\hat{p}_i(n)$ where $\hat{p}_i(n)$ is the power estimate of $x_i(n)$. The use of power-normalized step-sizes in the adaptation of the coefficients of the different subfilters increases significantly the convergence speed of the adaptation algorithm for colored input signals when compared to the speed of the conventional LMS algorithm (see Section 5).

2.2 Computational Complexity

The major advantage of the adaptive subband structure of Fig. 1 is the improvement in the convergence rate which can be achieved for high-correlated input signals, while keeping the low computational complexity of the LMS algorithm. In this section, we compare the number of multiplications required by the proposed subband structure with those required by the full-band and generalized transform-domain LMS algorithm.

The analysis filter bank of Fig. 1 can be efficiently implemented using the cosine modulation method in which only a prototype filter and a discrete cosine transform (DCT) are computed [18]. In such case, the overall number of multiplications per input sample required by the proposed subband structure is

$$N_{mult} = 2(N_S + N_P - M) + N_P + N_{DCT} \quad (10)$$

with the first term corresponding to the filtering and adaptation of the subfilters $G_k(z)$, the second term corresponding to the implementation of the prototype filter, and the last term corresponding to the computation of the DCT. Since the DCT is calculated for every new sample of the input, a recursive method with complexity of order M can be employed (i.e., $N_{DCT} \approx \mathcal{O}(M)$). For high-order adaptive filters, the dominant term in the above expression is $2N_S$, which is equal to the number of multiplications required by the full-band LMS algorithm. The transform-domain LMS algorithm with the DCT requires

$$N_{mult} = 2N_S + N_{DCT}, \quad (11)$$

where now $N_{DCT} \approx \mathcal{O}(N_S)$. For $N_S >> M$ and $N_S >> N_P$, (11) is significantly larger than (10).

Although the proposed method increases memory requirements by a factor of M when compared to the LMS and transform-domain LMS algorithms, since M can be chosen arbitrarily (because it is not related to the impulse response length), such memory increase can be limited to make the algorithm implementation feasible in many applications.

3 Convergence Analysis

We study now the convergence properties of the subband structure of Fig. 1 when the coefficients are updated by the normalized LMS adaptation algorithm of Eq. (8). Let us define the augmented input vector as

$$\boldsymbol{x}_a(n) = \begin{bmatrix} x(n) & x(n-1) & \cdots & x(n-L) \end{bmatrix}^T, \quad (12)$$

where $L = N_P + M(K-1) - 1$, and $\boldsymbol{H}_i$ as the matrix of dimension $K \times L$ with the first row containing the N_P coefficients of the ith analysis filter $H_i(z)$ completed with $L - N_P$ zeros and the next rows given by the previous row circularly shifted to the right by M samples. Then, the vector $\boldsymbol{x}_i(n)$, containing the samples of the transformed signals which are weighted by the coefficients of $G_i(z^M)$, is given by

$$\boldsymbol{x}_i(n) = \begin{bmatrix} x_i(n) \\ x_i(n-M) \\ \vdots \\ x_i\left(n-(K-1)M\right) \end{bmatrix} = \boldsymbol{H}_i \boldsymbol{x}_a(n). \quad (13)$$

Using the above vector definitions and the following weight vectors

$$\boldsymbol{g}_i(n) = \begin{bmatrix} g_{i,0}(n) & g_{i,1}(n) & \cdots & g_{i,K-1}(n) \end{bmatrix}^T, \quad (14)$$

$$\boldsymbol{g}(n) = \begin{bmatrix} \boldsymbol{g}_0(n) & \boldsymbol{g}_1(n) & \cdots & \boldsymbol{g}_{M-1}(n) \end{bmatrix}^T, \quad (15)$$

the output of the adaptive structure can be written as

$$\begin{aligned} y(n) &= \sum_{i=0}^{M-1} \boldsymbol{g}_i(n)^T \boldsymbol{x}_i(n) = \sum_{i=0}^{M-1} \boldsymbol{g}_i(n)^T \boldsymbol{H}_i \boldsymbol{x}_a(n) \\ &= \boldsymbol{g}(n)^T \begin{bmatrix} \boldsymbol{H}_0 \\ \vdots \\ \boldsymbol{H}_{M-1} \end{bmatrix} \boldsymbol{x}_a(n) \quad (16) \end{aligned}$$

The update equation (8) in vector notation is then given by

$$\boldsymbol{g}(n+1)=\boldsymbol{g}(n)+\boldsymbol{\mu}[d(n-\Delta)-y(n)]\begin{bmatrix}\boldsymbol{H}_0\\ \vdots\\ \boldsymbol{H}_{M-1}\end{bmatrix}\boldsymbol{x}_a(n), \tag{17}$$

where

$$\boldsymbol{\mu} = \text{diag}\{\mu_0\boldsymbol{I}_K, \mu_1\boldsymbol{I}_K, \cdots, \mu_{M-1}\boldsymbol{I}_K\}. \tag{18}$$

Taking expected values of both sides of Eq. (17), using Eq. (16) and assuming stationarity and that the input vector $\boldsymbol{x}_a(n)$ and the weight vector $\boldsymbol{g}(n)$ at the same iteration are uncorrelated ("independence assumption" [17]), we have

$$E[\boldsymbol{g}(n+1)]=E[\boldsymbol{g}(n)]+\boldsymbol{\mu}\begin{bmatrix}\boldsymbol{H}_0\\ \vdots\\ \boldsymbol{H}_{M-1}\end{bmatrix}\{\mathbf{p}_{\boldsymbol{x}_a d} \\ -\mathbf{R}_{\boldsymbol{x}_a\boldsymbol{x}_a}\left[\boldsymbol{H}_0^T\cdots\boldsymbol{H}_{M-1}^T\right]E[\boldsymbol{g}(n)]\}, \tag{19}$$

where $\mathbf{R}_{\boldsymbol{x}_a\boldsymbol{x}_a} = E[\boldsymbol{x}_a(n)\boldsymbol{x}_a(n)^T]$ is the augmented input autocorrelation matrix, and $\mathbf{p}_{\boldsymbol{x}_a d} = E[\boldsymbol{x}_a(n)d(n-\Delta)]$ is the input-delayed desired response cross-correlation vector.

From Eq. (19), the convergence performance of the adaptive algorithm is governed by the eigenvalues of the matrix

$$\boldsymbol{R}=\boldsymbol{\mu}\begin{bmatrix}\boldsymbol{H}_0\mathbf{R}_{\boldsymbol{x}_a\boldsymbol{x}_a}\boldsymbol{H}_0^T & \cdots & \boldsymbol{H}_0\mathbf{R}_{\boldsymbol{x}_a\boldsymbol{x}_a}\boldsymbol{H}_{M-1}^T\\ \vdots & \ddots & \vdots\\ \boldsymbol{H}_{M-1}\mathbf{R}_{\boldsymbol{x}_a\boldsymbol{x}_a}\boldsymbol{H}_0^T & \cdots & \boldsymbol{H}_{M-1}\mathbf{R}_{\boldsymbol{x}_a\boldsymbol{x}_a}\boldsymbol{H}_{M-1}^T\end{bmatrix}. \tag{20}$$

Therefore, having some knowledge of the input signal statistics, we can estimate the improvement in the convergence rate obtained with the structure of Fig. 1. Such analysis results can also be used to select the best analysis filter bank of Fig. 1, for a given input signal.

4 Filter Bank Design

In this section we describe an optimization procedure to obtain the perfect reconstruction cosine modulated filter bank which results in the best convergence rate for a given input signal second-order statistics when used in the structure of Fig. 1. Assuming that $p(n)$ is the impulse response of an N_P-length prototype filter $P(z)$ of an M-band cosine modulated filter bank, the analysis filters are [13]

$$h_k(n)=2p(n)\cos\left[\frac{\pi}{M}(k+\frac{1}{2})(n-\frac{N_P-1}{2})+\theta_k\right] \tag{21}$$

where $\theta_k = (-1)^k\frac{\pi}{4}$, for $0 \le k \le M-1$ and $0 \le n \le N_P - 1$. The necessary and sufficient conditions that a linear-phase prototype filter of length $N_P = 2mM$ has to satisfy in order to guarantee perfect reconstruction, for M even, are given by [14]

$$P_k(z^{-1})P_k(z)+P_{M+k}(z^{-1})P_{M+k}(z) = \frac{1}{2M} \tag{22}$$

for $0 \le k \le \frac{M}{2} - 1$, where $P_k(z)$ are the type 1 polyphase components of $P(z)$. Such constraints can be written in a quadratic form in terms of the prototype filter coefficients (taking into account the symmetry in the coefficients) [15] as follows:

$$\boldsymbol{p}^T\left[\boldsymbol{V}_k\boldsymbol{J}\boldsymbol{D}_n\boldsymbol{V}_k^T+\boldsymbol{V}_{M+k}\boldsymbol{J}\boldsymbol{D}_n\boldsymbol{V}_{M+k}^T\right]\boldsymbol{p} = \begin{cases} 0 & ,0\le n\le m-2\\ \frac{1}{2M} & ,n=m-1\end{cases} \tag{23}$$

where

$$\boldsymbol{p} = [p(0) \quad p(1) \quad \cdots \quad p(mM-1)]^T, \tag{24}$$

$$[\boldsymbol{V}_k]_{i,j}=\begin{cases}1, & i=k+2jM,\ k+2jM<mM\\ 1, & i=2M(m-j)-1-k,\ k+2jM\ge mM\\ 0, & \text{otherwise}\end{cases} \tag{25}$$

$$\boldsymbol{J} = \begin{pmatrix} 0 & \dots & 1\\ \vdots & \ddots & \vdots\\ 1 & \dots & 0\end{pmatrix}, \tag{26}$$

$$[\boldsymbol{D}_n]_{i,j} = \begin{cases}1, & n=i+j\\ 0, & \text{otherwise}\end{cases} \tag{27}$$

with $0 \le k \le \frac{M}{2}-1$ and $0 \le n \le m-1$. The dimensions of $\boldsymbol{p}$, $\boldsymbol{V}_k$, $\boldsymbol{J}$ e $\boldsymbol{D}_n$ are $mM\times 1$, $mM\times m$, $m\times m$ and $m\times m$, respectively. The above constraints are used in the quadratic-constrained least squares (QCLS) approach [15], with cost function given by the prototype filter stopband energy.

In order to reduce the convergence time of the adaptation algorithm of Eq. (8), the filter bank coefficients can be selected by a quadratic-constrained least squares optimization procedure, with cost function given by

$$\xi = \left[\frac{\lambda_{max}(\boldsymbol{R})}{\lambda_{min}(\boldsymbol{R})} - 1\right] \tag{28}$$

and quadratic constraints given by Eq. (23). The matrix $\boldsymbol{R}$ of Eq. (20) has dimension $MK\times MK$, which is large for a high order unknown system, resulting in an optimization problem of high complexity and processing time. However, in practice, we have verified that the optimization can be performed with a lower dimension matrix (i.e, considering a smaller number of adaptive coefficients K) without significant modification in the final prototype coefficients.

Algorithm	$\lambda_{max}(\boldsymbol{R})/\lambda_{min}(\boldsymbol{R})$
LMS	346.64
DCT	49.63
AFBS-QCLS	29.21
AFBS-Opt.	14.19

Table 1: Corresponding eigenvalue ratios for the simulations of Fig. 3

5 Simulation Results

Computer simulations are presented in order to illustrate the convergence behavior of the adaptive filter bank structure investigated in this paper. In the first experiment, the identification of a length $N_S = 128$ FIR system (with coefficients randomly obtained from samples of Gaussian white noise) is considered, with input signal generated by passing a white noise sequence by a first-order IIR filter with pole located at $z = 0.9$. The adaptive filter bank structure was simulated with $M = 8$ subbands, employing cosine modulated analysis filter banks with prototype filters of length $N_P = 16$ designed by the optimization procedure described in Section 4 (AFBS-Opt.) and by the quadratic constrained least-squares approach with stopband energy minimization (AFBS-QCLS). Each sparse subfilter contained $K = 17$ non-zero coefficients. In the prototype design method of Section 4, a matrix $\boldsymbol{R}$ of reduced dimension 72×72 (considering $K = 9$ instead of $K = 17$) was used in order to decrease the computational complexity of the optimization procedure. The step-size for each subfilter was inversely proportional to the power of the corresponding transformed signal $x_i(n)$, i.e.,

$$\mu_i(n) = \mu/\hat{p}_i(n) \tag{29}$$

with

$$\hat{p}_i(n) = 0.9\hat{p}_i(n-1) + 0.1x_i^2(n) \tag{30}$$

and $\mu = 0.5/(KM)$ in all simulations. Figure 3 presents the mean-square error (MSE) evolution of the adaptive filter bank structure with both prototype filters, of the conventional normalized LMS algorithm (LMS) and of the generalized transform-domain algorithm with a cosine transform of size 8 (DCT). Table 1 contains the eigenvalue ratios of the corresponding autocorrelation matrices $\boldsymbol{R}$ (Eq. (20)). It can be observed from the experimental results of Fig. 3 that the filter bank structure has significantly better performance than the LMS and the generalized transform-domain (DCT) algorithms, as expected from the theoretical analysis results of Table 1. The design of the filter bank according to Section 4 improves significantly the convergence performance of the filter bank structure.

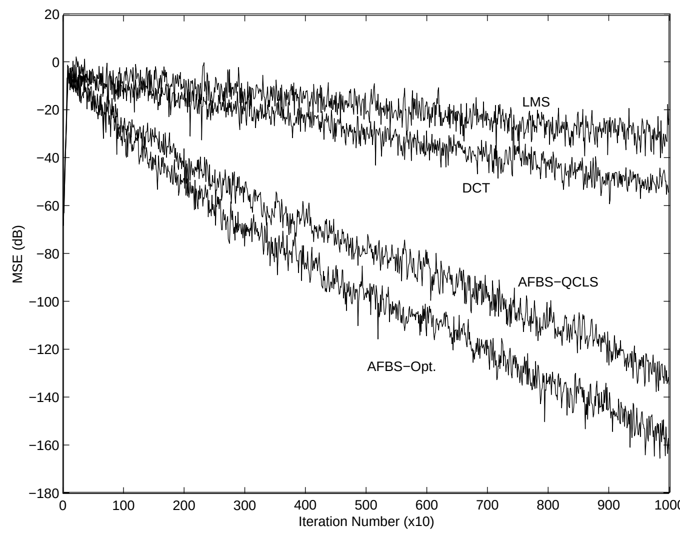

Figure 3: Results for the system identification experiment.

Another experiment with the adaptive filter bank structure and with the full-band LMS algorithm was carried out for echo canceling in a teleconference room. The microphone and loudspeaker signals were sampled at 8KHz. The filter bank structure was simulated with $M = 8$ subbands, using the same optimized cosine modulated filter bank of the system identification experiment. In order to implement a length $N_S = 1,200$ impulse response, $K = 151$ coefficients were used in each subband. To visualize the improvement obtained with the filter bank structure, the residual echo was decomposed in four subbands. In the low frequency band, the LMS and the AFBS algorithms had the same performance. However, in the other frequency bands, the residual echo of the AFBS was significantly smaller, as can be seen in Fig. 4 for the third subband. The delay introduced by the AFBS was of only 8 samples (1ms) and the computational complexity was slightly higher than that of the LMS algorithm (60 more multiplications).

6 Conclusions

We investigated, in this paper, the convergence properties of an adaptive filter structure which employs filter banks and sparse subfilters. The conditions on the filter bank and adaptive subfilter length were derived such that the structure becomes capable of exactly modeling any FIR system. The convergence behavior of the proposed adaptive structure was analyzed, and an optimization method based on this analysis

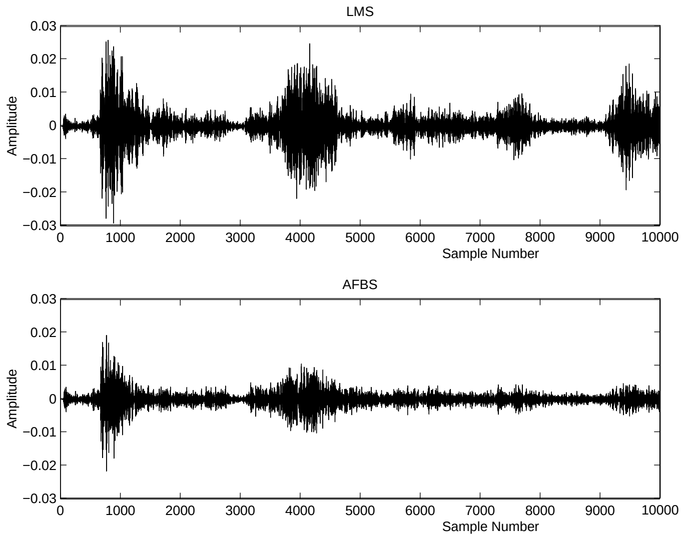

Figure 4: Results for the acoustic echo cancelling experiment: residual echo for the LMS (top) and AFBS (bottom).

was described for the design of the prototype filter of a cosine modulated filter bank. Computer simulations were presented in order to compare the performance of the proposed structure to those of previously proposed algorithms. It was shown that besides exactly modeling, significant convergence improvement can be obtained with the proposed structure for colored input signals.

References:

[1] A. Gilloire, Experiments with sub-band acoustic echo cancellers for teleconferencing, *Proc. IEEE Int. Conf. Acoust., Speech, Sig. Proc.*, pp. 2141-2144, Dallas, TX, Apr. 1987.

[2] H. Yasukawa, S. Shimada, and I. Furukawa, Acoustic echo canceller with high speech quality, *Proc. IEEE Int. Conf. Acoust., Speech, Sig. Proc.*, pp. 2125-2128, Dallas, TX, Apr. 1987.

[3] A. Gilloire and M. Vetterli, Adaptive filtering in subbands with critical sampling: analysis, experiments, and application to acoustic echo cancellation, *IEEE Trans. Signal Processing*, pp. 1862-1875, vol. 40, no. 8, Aug. 1992.

[4] M. Tahernezhadi, J. Liu, and X. Kong, An improved subband acoustic echo canceller for teleconferencing applications, *37th Midw. Symp. Circ. Syst.*, pp. 1424-1427, Aug. 1994.

[5] W. Kellermann, Analysis and design of multirate systems for cancellation of acoustical echoes, *Proc. IEEE Int. Conf. Acoust., Speech, Sig. Proc.*, pp. 2570-2573, New York, NY, Apr. 1988.

[6] M. R. Petraglia and S. K. Mitra, Performance analysis of adaptive filter structures based on subband decomposition, in *Proc. IEEE Int. Symp. Circ. Syst.*, pp. 60-63, Chicago, IL, May 1993.

[7] A. P. R. Rodrigues, M. R. Petraglia, and J. Szczupak, An adaptive subband structure with critical sampling, *Proc. IEEE Int. Symp. on Circuits and Systems*, pp. 368-371, Atlanta, GA, May 1996.

[8] S. S. Narayan, A. M. Peterson, and M. J. Narasimha, Transform domain LMS algorithm, *IEEE Trans. Acoust., Speech, Sig. Proc,*, vol. ASSP - 31, pp. 609-614, Jun. 1983.

[9] M. R. Petraglia and S. K. Mitra, Adaptive FIR filter structure based on the generalized subband decomposition of FIR filters, *IEEE Trans. Circuits and Systems II: Analog and Digital Signal Processing*, vol. 40, pp. 354-362, Jun. 1993.

[10] M. R. Petraglia and S. K. Mitra, An adaptive filter bank structure for adaptive line enhancement and channel equalization applications, in *Proc. SBT/IEEE Int. Telecommunications Symp.*, Rio de Janeiro, Brazil, pp. 1-5, Aug. 1994.

[11] B. E. Usevitch and M. T. Orchard, Adaptive filtering using filter banks, *IEEE Trans. Circuits and Systems II: Analog and Digital Signal Processing*, vol. 43, pp. 255-265, Mar. 1996.

[12] M. de Courville and P. Duhamel, Adaptive filtering in subbands using a weighted criterion, *IEEE Trans. Signal Processing*, pp. 2359-2371, Sep. 1998.

[13] G. Strang and T. Nguyen, *Wavelets and Filter Banks*, Wellesley - Cambridge Press, 1996.

[14] R. D. Koilpillai and P. P. Vaidyanathan, Cosine-modulated FIR filter banks satisfying perfect reconstruction, *IEEE Trans. Signal Processing*, pp. 770-783, Apr. 1992.

[15] T. Q. Nguyen, Digital filter banks design - quadratic constrained formulation, *IEEE Trans. Signal Processing*, vol. 43, pp. 2103-2108, Sep. 1995.

[16] P. P. Vaidyanathan, *Multirate Systems and Filter Banks*, Prentice-Hall, Englewood Cliffs, New Jersey, 1993.

[17] S. Haykin, *Adaptive Filter Theory*, 3rd ed., Prentice-Hall, Englewood Cliffs, New Jersey, 1996.

[18] H. S. Malvar, *Signal Processing with Lapped Transforms*, Artech House, 1992.